Radiology Case Reports 18 (2023) 386–391

Available online at www.sciencedirect.com

ScienceDirect

journal homepage: www.elsevier.com/locate/radcr

Case Report

Imaging features of a myoepithelial carcinoma of the nasal cavity: A case report and literature review ☆

Takayoshi Shinya, MD, PhD[a,], Tomoki Matsushita, MD[a], Yuka Hiroshima, MD[a], Yoichi Otomi, MD, PhD[a], Yasuhisa Kanematsu, MD, PhD[b], Yoshimi Bando, MD, PhD[c], Hisanori Uehara, MD, PhD[c], Yoshiaki Kitamura, MD, PhD[d], Masafumi Harada, MD, PhD[a]*

[a] *Department of Radiology, Tokushima University Hospital, 3-18-15, Kuramoto-cho, Tokushima City, Tokushima, 770-8503, Japan*

[b] *Department of Neurosurgery, Tokushima University Graduate School of Biomedical Sciences, Tokushima University, 2-50-1, Kuramoto-cho, Tokushima City, Tokushima, 770-8503, Japan*

[c] *Division of Pathology, Tokushima University Hospital, 2-50-1, Kuramoto-cho, Tokushima City, Tokushima, 770-8503, Japan*

[d] *Department of Otolaryngology, Tokushima University Graduate School of Biomedical Sciences, 2-50-1, Kuramoto-cho, Tokushima City, Tokushima, 770-8503, Japan*

ARTICLE INFO

Article history:
Received 10 October 2022
Accepted 23 October 2022

Keywords:
Myoepithelial carcinoma
Hemorrhagic necrosis
Nasal cavity
Magnetic resonance imaging
Computed tomography
Positron emission tomography

ABSTRACT

Myoepithelial carcinoma of the nasal cavity is extremely rare. We report the case of a 66-year-old man with myoepithelial carcinoma of the nasal cavity. Computed tomography (CT) and magnetic resonance imaging revealed a lobulated soft tissue mass with central necrosis and hemorrhage, as well as an invasion of the skull base and left orbit. The patient presented with continuous nasal congestion and heavy head and had no elevated level of squamous cell carcinoma-related antigen. CT, magnetic resonance imaging, or ^{18}F-fluorodeoxyglucose (FDG) positron emission tomography/CT revealed no evidence of a metastatic lesion. ^{18}F-FDG accumulation in the tumor was inhomogeneous and moderate. Histopathological examination of the resected specimen confirmed a well-circumscribed solid tumor with septa, a small area of hemorrhage, and necrosis. The subsequent diagnosis was a myoepithelial carcinoma of the left nasal cavity. This case shows that nasal myoepithelial carcinoma might appear as a well-defined lobulated mass with hemorrhagic necrosis and intense contrast enhancement in the solid component. We conjecture that hemorrhagic necrosis and intense enhancement values may be potential markers of nasal myoepithelial carcinoma.

☆ Competing Interests: None of the authors have any relevant conflict of interest or industry support related to this report.

* Corresponding author.
E-mail address: midnight-2005@nifty.com (T. Shinya).

https://doi.org/10.1016/j.radcr.2022.10.081

Introduction

Myoepithelial cells are physiologically important components of the glandular acini and ducts, and tumors arising from these cells are rare. Most tumors are benign, known as myoepitheliomas, but some are malignant. The latter entity has been termed malignant myoepithelioma or myoepithelial carcinoma [1,2]. Myoepithelial carcinoma is a rare malignancy predominantly derived from the salivary glands and palate. Although myoepithelial carcinoma is extremely rare, the nasal cavity can be the primary site of myoepithelial carcinoma [3]. To the best of our knowledge, magnetic resonance imaging (MRI) features of nasal myoepithelial carcinoma have been limited to 2 cases: T1-weighted image (T1WI) and T2-weighted image (T2WI) [3,4]. Therefore, the MRI features of nasal myoepithelial carcinoma have not been investigated, and no case of myoepithelial carcinoma of the nasal cavity with the features of computed tomography (CT) and ^{18}F-fluorodeoxyglucose (FDG) positron emission tomography (PET)/CT has been reported in the English literature.

We report a case of myoepithelial carcinoma in the nasal cavity and the features on MRI, CT, and ^{18}F -FDG PET/CT with a review of the literature.

Case report

A 66-year-old man underwent a whole-body CT scan after a fall half a year prior, and the CT scan incidentally revealed a mass occupying the left nasal cavity. He had a history of continuous nasal congestion and a heavy head for half a year before the accident. Nasal endoscopic examination revealed a polypoid mass in the left middle meatus, causing rightward deviation of the nasal septum. A physical examination revealed no neck lymph node swelling. The results of laboratory investigations, including the levels of squamous cell carcinoma-related antigen, were within normal limits.

Unenhanced CT revealed a 49 × 40 × 39 mm lobulated and heterogeneous hypodense tumor (Fig. 1a). Contrast-enhanced CT showed a well-enhanced lobulated tumor with the destruction of the skull base and lamina papyracea (Fig. 1b). No lymph node enlargement or distant metastases to other organs occurred.

MRI revealed a 53 × 50 × 39 mm lobulated nasal mass with invasion into the skull base and left orbit. On T2WIs, the tumor mainly had a high-signal intensity (SI) area, with an irregular central low-SI area (Fig. 2a). The tumor also had a low-SI septum and fibrous tissue on T2WIs (Fig. 2b). On T1WIs, the tumor mainly showed iso-SI compared to that of the muscle with a central high-SI area (Fig. 2c). Moderate- and high-intensity areas were observed in the sphenoid sinus on T1WIs, corresponding to mucus retention (Fig. 2c). Axial fat-saturated T1WIs revealed no fat components in the tumor (not shown).

On contrast-enhanced T1WIs, the tumor showed markedly intense contrast enhancement in the solid parts and septum within the tumor (Fig. 2d). In contrast, the central area showed no contrast enhancement, corresponding to hemorrhagic necrosis within the tumor (Fig. 2e). Diffusion-weighted images showed that the tumor had low- and high-SI areas (Fig. 2f). The apparent diffusion coefficient map of the same region (b = 1000 s/mm^2) showed no significant restricted diffusivity (Fig. 2g).

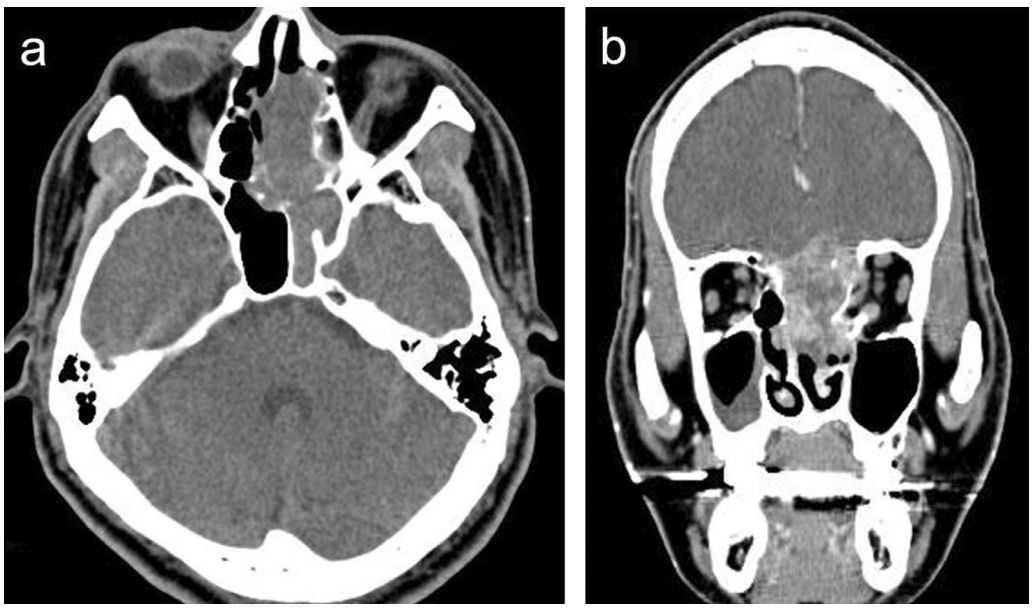

Fig. 1 – Computed tomography (CT) scans (soft tissue window). (a) Unenhanced axial CT reveals a lobulated hypodense nasal tumor with no calcification. (b) The coronal contrast-enhanced CT reveals the inhomogeneous well-enhanced tumor with the destruction of skull base and left lamina papyracea with the tumor.

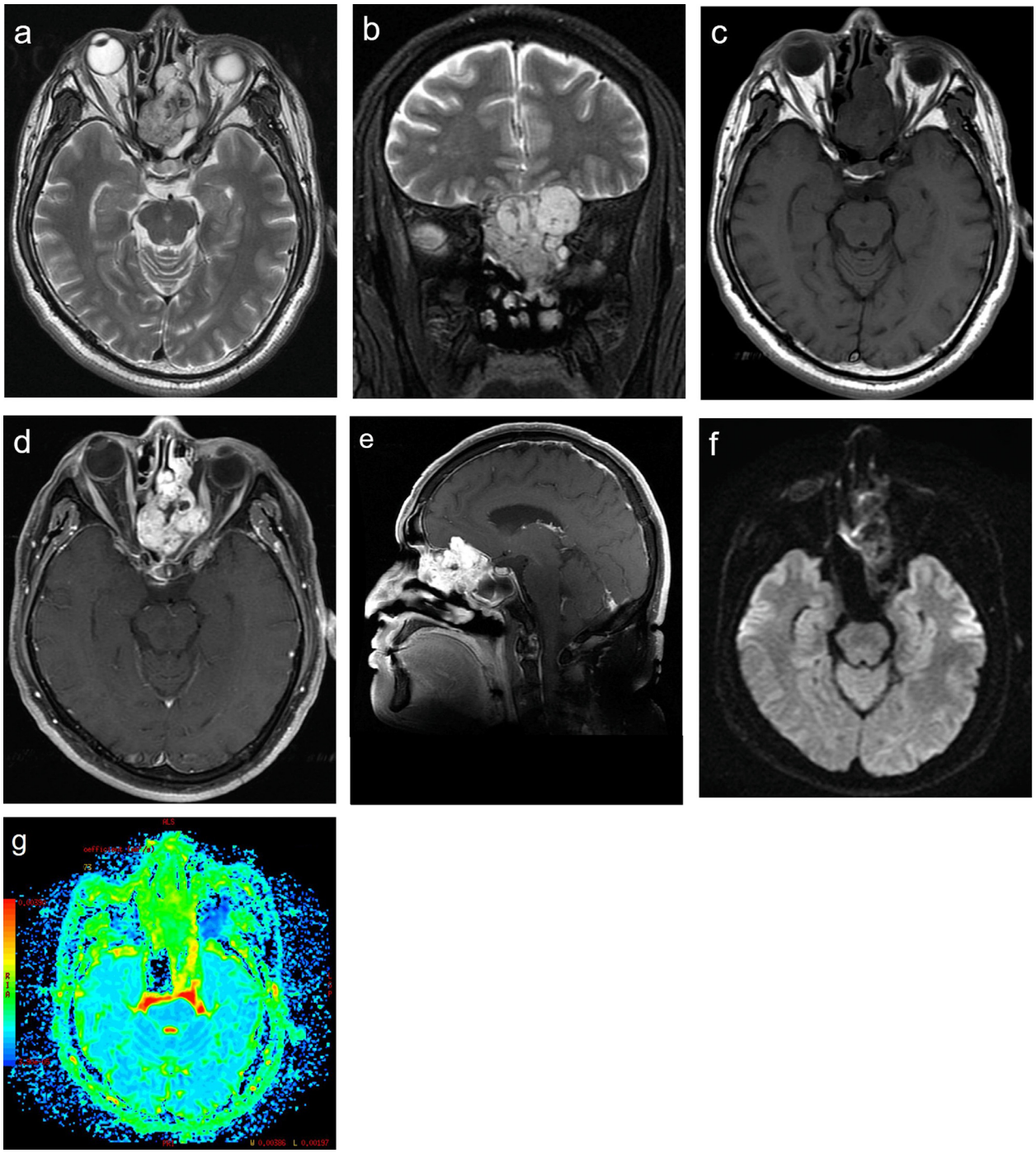

Fig. 2 – Magnetic resonance imaging (MRI). (a) The main parts of the tumor have high-signal intensity (SI) area with an irregular central low-SI area (arrow) on axial T2-weighted images (T2WIs) (repetition time [TR]/time/effective echo time [TE], 5000/98 ms). (b) Coronal T2WIs also reveal low-SI linear structures corresponding to the septum and fibrous tissue in the tumor. (c) The tumor has mainly an isointense area compared to that of the muscle with a slightly hyperintense central area (arrowhead) on axial T1-weighted images (T1WIs) (TR/TE, 667/10 ms). Homogeneous moderate- and high-intensity areas are observed in the sphenoid sinus on T1WIs, corresponding to mucus retention (arrow). (d) The tumor shows mainly inhomogeneous intense enhancement on axial contrast-enhanced T1WIs. (e) Sagittal contrast-enhanced T1WIs reveal the central area of the tumor with no contrast enhancement (arrowhead), corresponding to hemorrhagic necrosis (TR/TE, 467/10 ms). (f) Diffusion-weighted images show that most parts of the tumor have low and high signal intensities with peripheral high linear signal intensity corresponding to the artifact (TR/TE, 10000/88, b-value = 1000 s/mm^2). (g) The mean apparent diffusion coefficient of the tumors was 1.43 x 10^{-3} mm^2/s (b = 1000 s/mm^2).

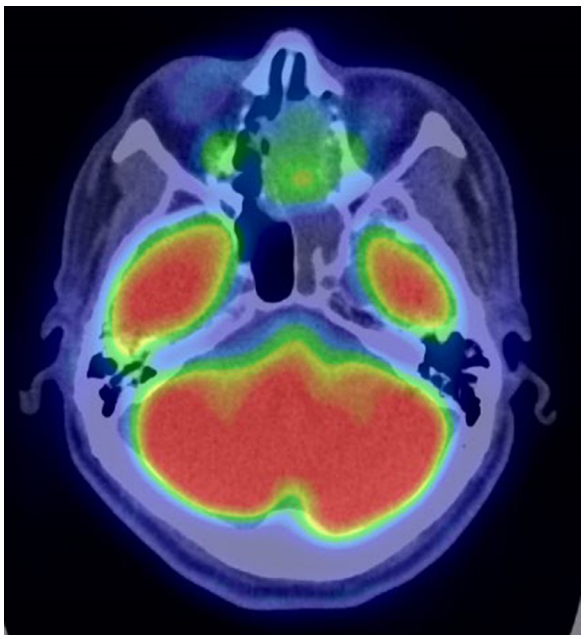

Fig. 3 – The positron emission tomography (PET/CT). The PET/CT image shows inhomogeneous increased accumulation of ^{18}F-FDG in the tumor. The maximum standardized uptake value for nasal tumor was 3.5.

PET/CT imaging was performed for further image evaluation and revealed a nasal mass with inhomogeneous increased accumulation of ^{18}F-FDG and no abnormal accumulation in other regions or lymph nodes (Fig. 3). The maximum standardized uptake value (SUVmax) of the nasal tumor was 3.5, suggesting its low-grade malignancy.

Various preoperative differential diagnoses of benign and malignant conditions were based on nonspecific CT and MRI features and FDG accumulation in the tumor. Therefore, an accurate preoperative diagnosis based on imaging alone is challenging.

The tumor was excised using a combined endoscopic endonasal and transcranial approach. The tumor mass had invaded the surrounding pachymeninx. It had a clear margin on the left middle nasal concha that could be completely dissected. Microscopically, the tumor invaded the surrounding bone tissue with an intratumoral hemorrhage. Most tumor cells appeared as round and spindle-shaped atypical cells with prominent nuclei and mitoses arranged in nests. No biphasic ductal and myoepithelial patterns were observed. Hyalinization and mucinous stroma were also observed (Fig. 4). Immunohistochemical analysis revealed that the tumor cells were positive for S-100 protein, cytokeratin (AE1/AE3), p63, and α-smooth muscle actin and focally positive for epithelial membrane antigen and CD117. The tumor cells were not immunoreactive for monoclonal antibodies against carcinoembryonic antigen and glial fibrillary acidic protein. The MIB-1 labeling index was scored as 60%, as the percentage of positive nuclei divided by the number of nuclei scored. These pathological findings led to a diagnosis of myoepithelial carcinoma of the nasal cavity.

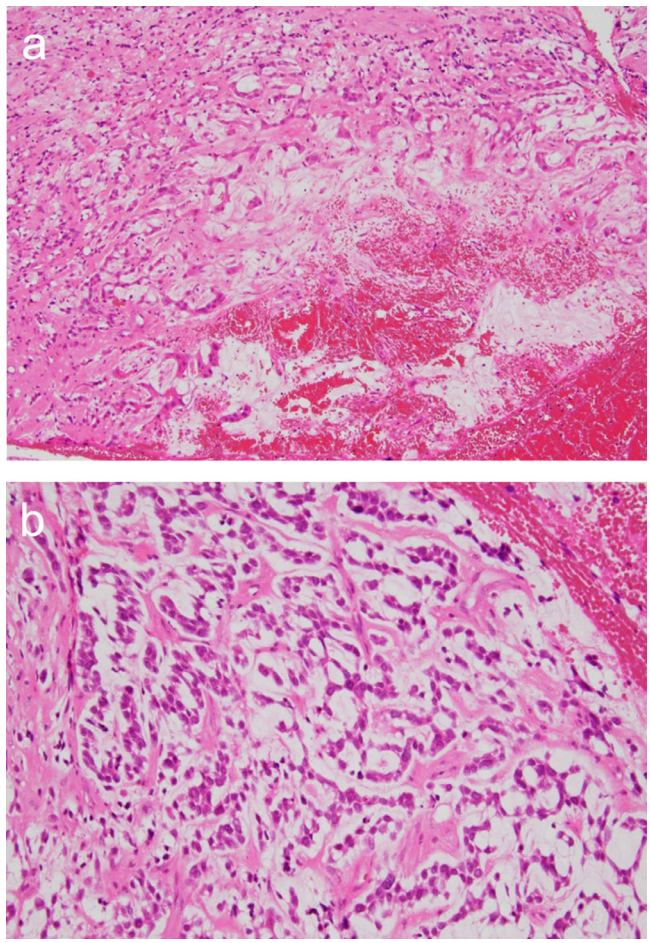

Fig. 4 – Histopathological findings of the surgical specimen. (a, b) Microscopically, hematoxylin-eosin staining shows round- and spindle-shaped atypical cells with intratumoral hemorrhage (a: low magnification, b: high magnification; hematoxylin and eosin staining).

Discussion

Myoepithelial carcinoma is a rare malignant epithelial tumor composed of atypical myoepithelial cells with increased mitotic activity and aggressive growth [5]. Myoepithelial carcinoma has been reported to infiltrate the surrounding tissue and even metastasize [6]. The tumor typically arises from benign lesions, such as pleomorphic adenomas, and less commonly from myoepitheliomas. In contrast, tumors also arise de novo [1,2].

The imaging characteristics of myoepitheliomas and myoepithelial carcinomas of the nasal cavity have not been well described. In the published cases for nasal myoepitheliomas [7–10], the CT showed nasal soft tissue densities with or without deviated nasal septum. Contrast enhancement by contrast medium varies from case to case and has no constant tendency for the contrast effect on contrast-enhanced CT [7,9,10]. In a case report with MRI findings, nasal myoepithelioma had a heterogeneous high SI on T2WI [9]. In another case, MRI showed a nasal myoepithelioma with well-defined margins

with heterogeneous high SI on T2WI and low SI on T1WI, with moderate enhancement on T1WI with gadolinium [7]. On the other hand, in the previous case of a high-grade myoepithelial carcinoma in the nasal cavity, the T1WI shows a 2 cm irregular tumor in the left anterior nasal cavity without invasion to the septum, hard palate, left maxillary sinus, and nasopharynx and without locoregional metastasis [3]. In another report on anaplastic myoepithelial carcinoma, T2WI revealed a 54 mm lobulated tumor of the sinonasal tract with heterogeneous high SI [4]. In the present case, unenhanced CT showed a lobulated and heterogeneous hypodense tumor in the left nasal cavity, with bone destruction and involvement of the skull base and lamina papyracea. The nasal tumor appeared as a well-enhanced tumor on contrast-enhanced CT. On MRI, most parts of the tumor showed a high SI on T2WI, with markedly intense contrast enhancement on contrast-enhanced T1WI, corresponding to the solid parts of the tumor. The central part of the tumor, corresponding to hemorrhagic necrosis, showed low SI on T2WI. The intratumoral septum showed a low SI on T2WIs.

Although reports on the imaging findings of myoepithelial carcinoma in the head and neck regions are limited, CT and MRI revealed exophytic lobulated masses in the nasopharynx protruding into the nasal cavities [4,5]. MRI revealed lobulated tumors with heterogeneous high SI on T2WIs in patients with myoepithelial carcinomas in the nasopharynx, right rhinopharynx, and left submandibular region [2,3,11]. In myoepithelial carcinoma of the soft tissue and bone, DWI shows high intensities and low ADC values [12,13]. However, DWI and ADC values for head and neck myoepithelial carcinoma have not been previously reported. In the present case, the nasal tumor had low- and high-SI areas on DWI, and the ADC map of the region showed no significant restricted diffusivity. Therefore, the detailed enhancement pattern of nasal myoepithelial carcinoma and the typical ADC values remain unclear. These findings may indicate that lobular morphology, invasion of the surrounding tissue beyond the bone structure, and intratumoral hemorrhage on T2WI and contrast-enhanced T1WI may be potential imaging markers suggestive of nasal myoepithelial carcinomas, which need to be assessed in further investigations. In contrast, the heterogeneity on T2WI and contrast enhancement on contrast-enhanced CT and MRI has limited roles in differentiating between myoepithelioma and myoepithelial carcinoma in the nasal cavity.

Several studies have reported ^{18}F-FDG FDG findings in patients with myoepithelial carcinomas in different organs [1,14–16]. In a patient with parotid myoepithelial carcinoma, ^{18}F-FDG PET/CT demonstrated ^{18}F-FDG accumulation with a SUVmax of 10.1 [15]. Myoepithelioma of the soft tissue had increased ^{18}F-FDG accumulation with a SUVmax of 6.07, suggesting a malignant lesion [16]. Previous studies have reported that ^{18}F-FDG PET/CT imaging demonstrated hypermetabolic lesions corresponding to myoepithelial carcinomas of the tongue and parapharyngeal space [1,17]. In contrast, pulmonary myoepithelial carcinoma had very subtle ^{18}F-FDG accumulation, with a SUVmax of 1.2 [14]. In the present case, the nasal myoepithelial carcinoma had an inhomogeneously increased ^{18}F-FDG accumulation with a SUVmax of 3.5. Therefore, in patients with myoepithelial carcinoma, the accurate correlation between ^{18}F-FDG accumulation and aggressive nature remains unclear, and future studies are needed to determine the diagnostic capacity of ^{18}F-FDG accumulation for the tumor aggressiveness of myoepithelial carcinoma.

In conclusion, nasal myoepithelial carcinoma presents as a lobulated mass with invasion of the surrounding tissues and a hemorrhagic region and shows low SI on T2WI, with markedly intense contrast enhancement in the solid parts and septum within the tumor. Although the diagnostic value of low SI on T2WI for nasal tumors has not been fully investigated, these can be potential markers for distinguishing benign from malignant tumors in the nasal cavity. Therefore, it is critical to consider the possibility of nasal myoepithelial carcinoma when examining nasal hemorrhagic tumors with lobulated morphology and high SI on contrast-enhanced MRI.

Funding

This research did not receive any specific grant from funding agencies in the public, commercial, or not-for-profit sectors.

Authors' contributions

Takayoshi Shinya designed this case report and wrote the initial draft of the manuscript. Tomoki Matsushita and Yuka Hiroshima contributed to the analysis of the imaging and assisted in the preparation of the manuscript. All other authors contributed to data analyses and data collection of imaging and pathologic specimens and critically reviewed the manuscript. All authors approved the final version of the manuscript and agree to be accountable for all aspects of the work in ensuring that questions related to the accuracy or integrity of any part of the work are appropriately investigated and resolved.

Patient consent

This study does not require institutional review board approval. Informed consent was obtained for the case report to be published.

Supplementary materials

Supplementary material associated with this article can be found, in the online version, at doi:10.1016/j.radcr.2022.10.081.

REFERENCES

[1] Nicholas RG, Hanson JA, Meiklejohn DA. Myoepithelial cell carcinoma of the oral tongue: case report and review of the literature. Clin Med Insights Oncol 2019;13:1179554919838254. doi:10.1177/1179554919838254.

[2] Magliulo G, Pulice G, Fusconi M, Cuiuli G. Malignant myoepithelioma of the rhinopharynx: case report. Skull Base 2005;15:113–16 discussion 117. doi:10.1055/s-2005-870596.
[3] Yingting M, Agaimy A, Wang S, Kuick CH, Chang KT, Petersson F. High-grade myoepithelial carcinoma can show histologically undifferentiated/anaplastic features. Ann Diagn Pathol 2018;37:20–4. doi:10.1016/j.anndiagpath.2018.09.004.
[4] Petersson F, Chao SS, Ng SB. Anaplastic myoepithelial carcinoma of the sinonasal tract: an underrecognized salivary-type tumor among the sinonasal small round blue cell malignancies? Report of one case and a review of the literature. Head Neck Pathol 2011;5:144–53. doi:10.1007/s12105-010-0226-y.
[5] Tuncel U, Ergul G, Ozlugedik S, Unal A. Myoepithelial carcinoma in the nasopharynx: an unusual localization. Yonsei Med J 2004;45:161–5. doi:10.3349/ymj.2004.45.1.161.
[6] Sayed SI, Kazi RA, Jagade MV, Palav RS, Shinde VV, Pawar PV. A rare myoepithelioma of the sinonasal cavity: case report. Cases J 2008;1:29. doi:10.1186/1757-1626-1-29.
[7] Nakaya K, Oshima T, Watanabe M, Hidaka H, Kikuchi T, Higashi K, et al. A case of myoepithelioma of the nasal cavity. Auris Nasus Larynx 2010;37:640–3. doi:10.1016/j.anl.2010.03.004.
[8] Gourh G, Arora RD, Hussain N, Nagarkar N. Myoepithelioma of nasal septum: a rare minor salivary gland tumour. BMJ Case Rep 2019;12:e230926. doi:10.1136/bcr-2019-230926.
[9] Fujikura T, Okubo K. Nasal myoepithelioma removed through endonasal endoscopic surgery: a case report. J Nippon Med Sch 2010;77:273–6. doi:10.1272/jnms.77.273.
[10] Ramesh D, Khong GC, Sumathi V. A case of myoepithelioma of the nasal cavity. Indian J Otolaryngol Head Neck Surg 2019;71(Suppl 3):1745–7. doi:10.1007/s12070-017-1093-6.
[11] Soon G, Petersson F. Myoepithelial carcinoma of the nasopharynx: report of a rare case and a review of the literature. Head Neck Pathol 2015;9:474–80. doi:10.1007/s12105-015-0638-9.
[12] Lin CH, Wu KY, Chen CK-H, Li CF, Hsieh TJ. Myoepithelial carcinoma of tibia mimic giant cell tumor: a case report with emphasis on MR features. Skelet Radiol 2019;48:1637–41. doi:10.1007/s00256-019-03198-w.
[13] Shinya T, Kojima Y, Monobe Y, Fujiwara H, Uehara S, Kato K. MRI and CT features of a malignant myoepithelioma of the scrotum: a case report and literature review. Radiol Case Rep 2021;16:2962–8. doi:10.1016/j.radcr.2021.07.013.
[14] Zhang Y, Li B, Hou J, Shi H. Primary myoepithelial carcinoma of the lung and 18F-FDG PET/CT. Rev Esp Med Nucl Imagen Mol (Engl Ed) 2018;37:175–7. doi:10.1016/j.remn.2017.04.006.
[15] Dekhou A, Rehman R, Parzen JS, Quinn TJ, Zhang PL, Rontal M, et al. Primary parotid tumor thrombosis: immunohistologic features and awareness of metastatic potential. Cureus 2021;13:e16174. doi:10.7759/cureus.16174.
[16] Hamada K, Ueda T, Tomita Y, Yoshikawa H, Hatazawa J. Myoepithelioma of soft tissue originating from the hand: 18F-FDG PET features. AJR 2006;186:270–1. doi:10.2214/AJR.05.0191.
[17] Chongjiao Li, Tian Y, Shen Y, Wen B, He Y. 18F-FDG PET/CT findings in a rare myoepithelial carcinoma arising in the parapharyngeal space. Clin Nucl Med 2020;45:894–5 18F. doi:10.1097/RLU.0000000000003242.